RESEARCH ARTICLE SUMMARY

AGING

Sex- and age-dependent genetics of longevity in a heterogeneous mouse population

Maroun Bou Sleiman†, Suheeta Roy†, Arwen W. Gao, Marie C. Sadler, Giacomo V. G. von Alvensleben, Hao Li, Saunak Sen, David E. Harrison, James F. Nelson, Randy Strong, Richard A. Miller, Zoltán Kutalik, Robert W. Williams*, Johan Auwerx*

INTRODUCTION: Aging is the progressive decline in physical, mental, and reproductive capacities that is accompanied by multiple morbidities and associated with increased mortality. Despite advances in identifying aging pathways and drugs that extend life span in model systems, an integrative understanding of the interplay between genetics, sex, and environment in aging and life-span determination is largely lacking.

RATIONALE: Although there is no single measure of aging, studies depend on surrogate or related traits such as longevity, life history, age-related disease onset, and physiological markers. Characterizing genetic and nongenetic determinants of longevity at the population level may identify genes and pathways involved in aging, providing avenues for targeted anti-aging therapies and extension of healthy longevity. We set out to query genetic regulators of longevity in a total of 3276 UM-HET3 mice used in longevity studies by the National Institute on Aging's Interventions Testing Program (NIA ITP). We interrogated whether the genetic basis of longevity is sex and age dependent, and whether nongenetic factors such as litter size and the effect of early access to nutrients on growth contribute to longevity determination. We characterized the age- and genotype-dependent changes in liver gene expression in mice from the same genetic cross. Finally, we integrated these results with orthogonal datasets to obtain a resource of prioritized candidate genetic loci and genes for further investigation.

RESULTS: When jointly analyzing males and females, we obtained a single, previously described, longevity locus on chromosome 12. However, when analyzed separately, males and females had distinct genetic determinants of longevity. In females, a single locus on chromosome 3 was uncovered, whereas in males, loci were detected only when early deaths were excluded, suggesting that some genetic variations had an effect on longevity beyond a certain age. Increased body weight associated with earlier death and some of the variation in adult body weight are explained by litter size. Hence, early access to nutrients may affect mouse longevity through its effect on growth. We used Mendelian randomization to replicate the relationships between early growth, adult size, and longevity in humans. To prioritize genes under the longevity loci, we profiled liver gene expression of adult and old mice to look for sex-, age-, and genetically driven differences in expression. Female livers had higher interferon-related gene expression, and older mice had overexpressed immune-related genes. Genetic regulation of gene expression was assessed, with the majority being conserved across sexes and age. We combined our results with data from multiple sources in model organisms and humans to compile an interactive resource for conserved longevity gene prioritization (https://www.systems-genetics.org/itp-longevity). Worm life-span experiments validated some of the most highly scoring genes and identified *Hipk1*, *Ddost*, *Hspg2*, *Fgd6*, and *Pdk1* as candidates.

CONCLUSION: This study provided insights into determinants of longevity, highlighting genetic mediators that can be sex or age specific, and nongenetic effects such as early access to nutrients. The combined body of information assembled from this study and the external data constitute a hypothesis-building resource for future studies on, and therapies for, aging, age-related disease, and longevity. ■

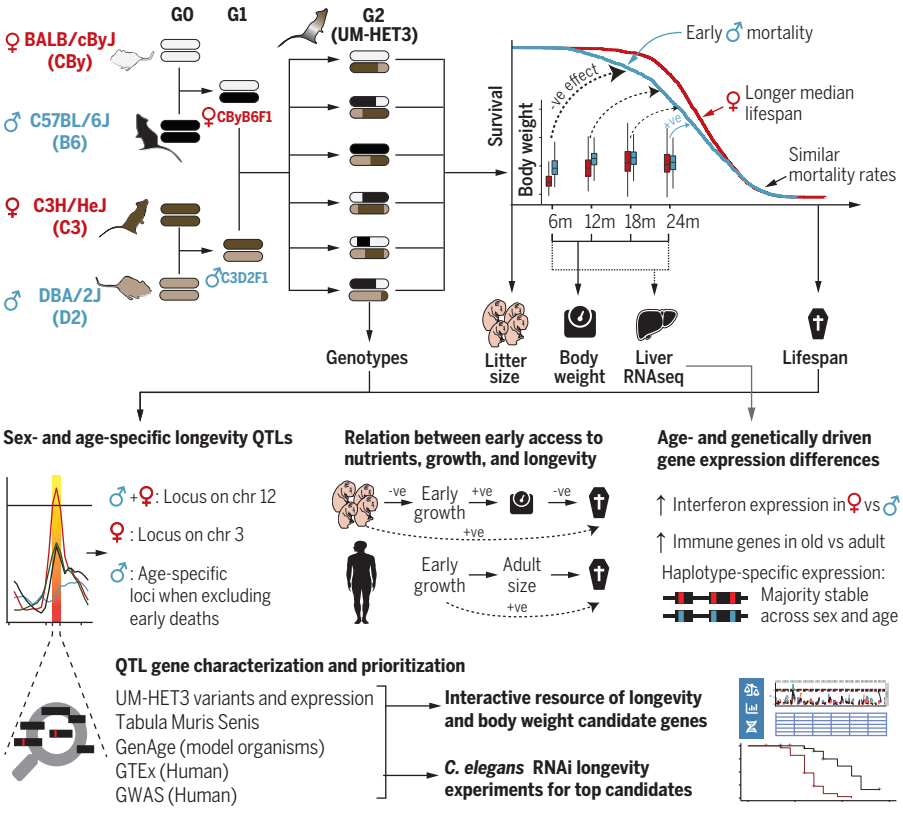

Genetic analyses in UM-HET3 mice used in the Interventions Testing Program highlight sex- and age-specific longevity loci. Body weight associates with longevity, as does litter size, through its effect on body weight. Mendelian randomization in humans recapitulated these relationships between early growth and life span. Gene expression analyses, cross-species integration, and *Caenorhabditis elegans* life-span experiments highlight candidate longevity genes and provide a resource for further investigation.

The list of author affiliations is available in the full article online.
*Corresponding author. Email: labwilliams@gmail.com (R.W.W.); admin.auwerx@epfl.ch (J.A.)
†These authors contributed equally to this work.
Cite this article as M. Bou Sleiman *et al.*, *Science* **377**, eabo3191 (2022). DOI: 10.1126/science.abo3191

RESEARCH ARTICLE

AGING

Sex- and age-dependent genetics of longevity in a heterogeneous mouse population

Maroun Bou Sleiman[1]†, Suheeta Roy[2]†, Arwen W. Gao[1], Marie C. Sadler[3,4,5], Giacomo V. G. von Alvensleben[1], Hao Li[1], Saunak Sen[6], David E. Harrison[7], James F. Nelson[8], Randy Strong[8,9], Richard A. Miller[10], Zoltán Kutalik[3,4,5], Robert W. Williams[2]*, Johan Auwerx[1]*

DNA variants that modulate life span provide insight into determinants of health, disease, and aging. Through analyses in the UM-HET3 mice of the Interventions Testing Program (ITP), we detected a sex-independent quantitative trait locus (QTL) on chromosome 12 and identified sex-specific QTLs, some of which we detected only in older mice. Similar relations between life history and longevity were uncovered in mice and humans, underscoring the importance of early access to nutrients and early growth. We identified common age- and sex-specific genetic effects on gene expression that we integrated with model organism and human data to create a hypothesis-building interactive resource of prioritized longevity and body weight genes. Finally, we validated *Hipk1*, *Ddost*, *Hspg2*, *Fgd6*, and *Pdk1* as conserved longevity genes using *Caenorhabditis elegans* life-span experiments.

Aging is a time-dependent functional decline in molecular, cellular, and organismal homeostasis that is affected by multiple environmental and genetic factors (*1*). Genetic studies, such as loss or gain of function or forward genetic screens, have identified many of its conserved genes and mechanisms (*2*, *3*). From the metabolic perspective, nutrient-sensing pathways such as the growth hormone and insulin-like growth factor axis (GH/IGF1), target of rapamycin (TOR), adenosine 5´-monophosphate (AMP)–activated protein kinase (AMPK), and sirtuins control aging or affect longevity (*1*, *3*). In addition to metabolic decline, other features such as loss of proteostasis, increased genome instability, changes in epigenetic marks, and alterations in telomere length have been proposed to promote aging (*1*, *4*, *5*). Here we used an unbiased genetic and molecular cross-species approach to highlight drivers of aging, starting with genetic mapping of loci that modulate variation in life span in a large multicenter and multiyear four-way intercross of male and female untreated control mice from the Interventions Testing Program (ITP).

[1]Laboratory of Integrative Systems Physiology, Institute of Bioengineering, École Polytechnique Fédérale de Lausanne, Lausanne 1015, Switzerland. [2]Department of Genetics, Genomics and Informatics, University of Tennessee Health Science Center (UTHSC), Memphis, TN 38163, USA. [3]Institute of Primary Care and Public Health (Unisante), University of Lausanne, Lausanne 1011, Switzerland. [4]Swiss Institute of Bioinformatics, Lausanne 1015, Switzerland. [5]Department of Computational Biology, University of Lausanne, Lausanne 1015, Switzerland. [6]Department of Preventive Medicine, University of Tennessee Health Science Center, Memphis, TN 38163, USA. [7]The Jackson Laboratory, Bar Harbor, ME 04609, USA. [8]Barshop Center for Longevity Studies at the University of Texas Health Science Center at San Antonio, San Antonio, TX 78229, USA. [9]South Texas Veterans Healthcare System, San Antonio, TX 78229, USA. [10]Department of Pathology, University of Michigan Geriatrics Center, Ann Arbor, MI 48109-2200, USA.
†These authors contributed equally to this work.
***Corresponding author. Email: labwilliams@gmail.com (R.W.W.); admin.auwerx@epfl.ch (J.A.)**

Multicenter and multiyear analysis identifies sex- and age-specific longevity loci

The ITP was funded by the National Institute on Aging starting in 2004 to test putative positive effects of dietary and drug interventions on life span (healthy aging) (*6*, *7*). For each intervention, a large and sex-balanced subcohort of control animals was aged until close to natural death along with the treated cases (*8*). All controls and cases were from a four-way intercross made by mating BALB/cByJ × C57BL/6J F_1 females—JAX Stock #100009—to C3H/HeJ × DBA/2J F_1 males—JAX Stock # 100004—the so-called UM-HET3 cross. Animals were bred at three independent testing sites (Jackson Laboratory, University of Michigan, and University of Texas Health Science Center at San Antonio) using F_1 animals from the Jackson Laboratory. The combination of a high level of genetic heterogeneity, very large family sample size, and balanced replication across sites has led to an unprecedented resource of longevity research (*9*). Tail biopsies were systematically collected from almost all mice, thus enabling the genotyping and subsequent genetic analyses presented here (*8*) (Fig. 1A).

We generated genotype data on 3276 mice, including 2356 control and 920 drug-treated mice (fig. S1, A and B, and data S1). The treated cases included animals subjected to 20 different drugs that had no population-level influence on longevity; this complexity renders the statistical inference of genetic and drug effects more challenging, and we therefore used this group in combination with the controls in supplementary quantitative trait locus (QTL) analyses. In addition to being a genetically heterogeneous panel with a wide range of variation in longevity and body weight, the cohort (year of birth) and site have effects on body weight and longevity (most prominently in males) despite all efforts of standardization (*10*) (fig. S1, C and D). To avoid biases due to these nongenetic effects, we accounted for center and year in all analyses.

As previously shown in the UM-HET3 cross (*10*), females have a higher median life span than males (female median = 886 days, 95% confidence interval (CI) [871–897], male median = 836 days, 95% CI [816–851]), with the largest difference in the survival curves attributable to increased early mortality in males between ages of about 300 and 800 days. Between 800 and 1000 days, females have a higher rate of mortality (fig. S1B). As of 1000 days, mortality rates are similar, indicating similar hazard rates at later ages and similar maximum longevity (fig. S1, A to C).

Given such age- and sex-specific hazards, we asked whether segregating loci affect life span in both sexes at all ages or whether sex- and age-specific effects are predominant (fig. S2). To determine whether genetic loci are sex specific, we performed four QTL mapping analyses: for each sex separately, and for the combined dataset with and without sex-by-genotype interaction term. To accommodate the multicenter and multiyear study design, we used mixed-effects Cox models with site and cohort as random effects and sex as fixed effect when appropriate. To assess the statistical significance of the results, we calculated empirical p values for the associations based on permutations (*8*) and characterized QTLs with $p < 0.2$.

A genome scan including both sexes identified a single QTL at chromosome 12, which may be a previously described locus in the UM-HET3 and BXD cohorts (Fig. 1B, data S2, and table S1) (*11*, *12*). We also detect one significant female-specific locus at chromosome 3 ($p = 0.006$) but no significant exclusive male loci. There is no evidence for sex-by-haplotype interaction, which may be related to power limitations due to sample size.

Early male mortality raised the possibility that some early pathologies or behavioral factors, possibly genetically driven, may mask genetic effects on longevity. Previously, this potential confounding was dealt with through removal of data from mice with early deaths, and this strategy has proven to be useful in identifying longevity-associated QTLs (*11*). We therefore performed successive QTL scans by removing increasing proportions of early deaths (Fig. 1C). To define peaks in these scans based on smaller subsets of the mice, we also relaxed the significance thresholds from 0.05 to 0.2. This approach revealed that the female chromosome 3

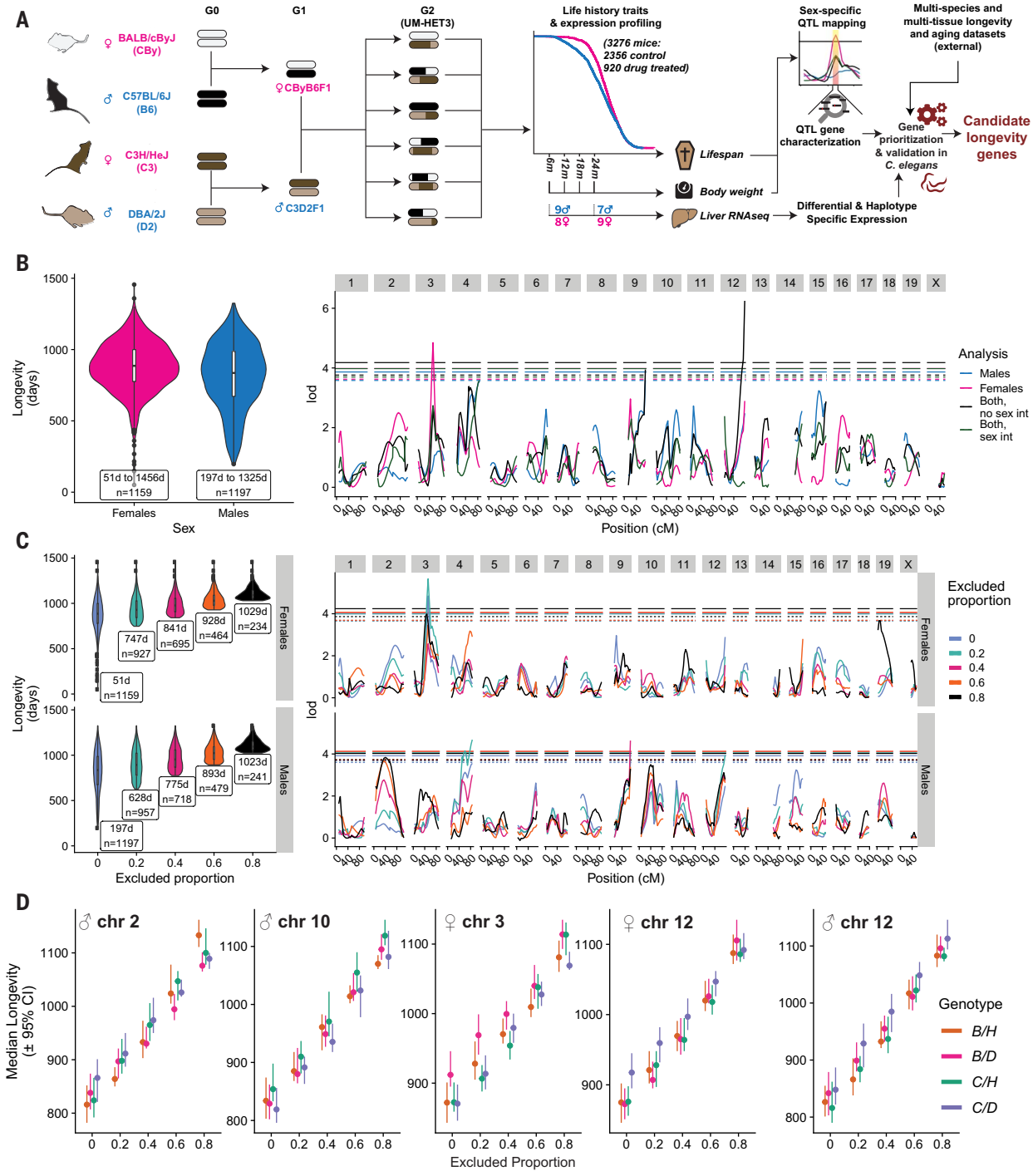

Fig. 1. QTL mapping of longevity identifies sex- and age-specific loci. (**A**) General scheme of the UM-HET3 four-way intercross and the end points examined in this study. The UM-HET3 mice come from a cross of a female (BALB/cByJ × C57BL/6J) F_1 and a male (C3H/HeJ × DBA/2J) F_1. The 3276 mice in this study are either controls (n = 2356) or were treated with 20 drugs that had no population-level effect on longevity (n = 920, data S1), from the NIA ITP conducted at two different sites (UT and UM) and spanning years 2004 to 2011. Natural life span, body weight, and DNA were collected from these mice. A separate UM-HET3 cohort (Glenn Center, UM) was used to obtain livers from young and old males and females for RNA sequencing to study sex- and age-related gene expression changes and haplotype-specific expression. (**B**) (Left) Distribution of female and male life spans. (Right) QTL mapping results for longevity in four analyses. The "Both, no sex int" includes all mice with sex as a fixed effect and site as a random effect and cohort year as a nested random effect within site. The "Both, sex int" tests for sex-by-haplotype interactions. The Male and Female models are restricted to one sex. Solid and dashed horizontal lines indicate permutation-based significance thresholds for α = 0.05 and 0.2, respectively. (**C**) QTL scans for life span performed after excluding different percentiles of mice that die early. (Left) Distribution of life-span values after exclusion of mice. The labels indicate the minimal life span in days and the number of mice. (Right) Overlaid QTL scans, colored by truncation level for females and males. Solid and dashed horizontal lines indicate permutation-based significance thresholds as in (B). (**D**) Median longevity of mice stratified by haplotype at male loci on chromosomes 2 and 10, female loci on chromosomes 3, and male and females at the chromosome 12 locus, after exclusion of different proportions of early deaths. Alleles *B*, *C*, *H*, and *D* correspond to CBy, B6, C3, and D2 strains, respectively.

QTL is robust to removal of early deaths as it only slightly decreased in significance (empirical p value = 0.006 and 0.081 when 0 and 80% of mice are removed, respectively) even upon removal of 80% of early deaths—that is, when only 20% of the longest-lived female mice were retained. One female-specific locus emerged on chromosome 19 only in the 20% of longest-lived females.

In contrast to females, multiple male loci increased in significance upon exclusion of early deaths. Specifically, the most significant locus is on chromosome 4 (at 20% truncation, empirical p value = 0.017) followed by less significant ones on chromosomes 2, 9, 10, and 12 (at 60, 20, 80, and 20% truncation, respectively; $0.05 < p < 0.2$). Upon observing the longevity distribution of mice carrying different allelic combinations at the chromosome 2 locus, we could appreciate how allelic effects become significant when early-death animals were progressively removed (Fig. 1D). Male mice carrying the *B/H* allele combination in the chromosome 2 locus do not differ from the whole male population ($p = 1$, Fig. 1D, left panel), but are the longest lived as we removed earlier deaths ($p = 0.137$ at 80% truncation). The age-specific and male-specific chromosome 10 locus ($p = 1$ and 0.185 at 0 and 80% truncation, respectively) overlaps with another previously described UM-HET3 longevity locus (*11*). The chromosome 12 locus detected in males overlaps with the one that we found in the analysis incorporating males and females and already identified in UM-HET3 (*11*). When examining sex-specific scans, the *C/D* allele combination offers an advantage in males (Fig. 1C, lowest empirical p value = 0.06 at 20% truncation in males) but not in females (Fig. 1C, lowest empirical p value = 0.357, no truncation).

To further explore whether QTLs overlap with known genetic associations, we looked for correspondence with known longevity, growth, and body size QTLs in the Mouse Genome Informatics database (*13*) (table S1). Except for the chromosome 10 and 12 loci in males, there is no overlap with longevity or life-span loci, which is not surprising given the general dearth of longevity QTLs likely due to limited power of existing studies. Instead, we found extensive overlap with known growth or body weight loci, pointing to the importance of genetic determination of growth rates on longevity.

Interplay between early growth, size, and longevity in mice and humans

The relation between growth, body size, and longevity has been extensively studied (*10*, *14*, *15*). This and our observation of overlap between longevity loci and growth QTLs prompted us to explore this relation further. At the phenotypic level, we observed an inverse relationship between early body weight and longevity that is more pronounced in males (Fig. 2, A and B). For instance, the hazard ratio of a 10-g increase at 6 months is ~1.8 and ~1.20 in males and females, respectively (mixed-effects Cox model p values < 0.00001 and 0.0016). This relation progressively decreased in magnitude, yet remained detectable until 18 months. At 24 months, the relation disappeared in females and reversed in males, suggesting that lower body weight at an advanced age (between 18 and 24 months) may be a predictor of earlier mortality in males as they lose weight prior to death. These observations are not only in agreement with studies in UM-HET3 mice (*10*, *14*) but also with findings in humans, in which higher childhood weight is associated with higher morbidity and mortality, especially in males (*16*, *17*), and weight loss at older ages is associated with increased frailty and mortality risk (*18*, *19*).

Before exploring the genetic determinants of body weight variation, we characterized the effects of nongenetic factors on body weight and whether they can contribute to variation in longevity in the UM-HET3 mice. Because the differences in body weight can be attributed to genetic and environmental factors, we wondered whether early access to nutrients as a result of litter size differences could affect growth, and consequently adult body weight and longevity (*20*). We used litter size information of a subset of 1575 control mice aged at the University of Texas, San Antonio. Indeed, a significant negative effect of litter size on male and female body weights at 6, 12, 18, and 24 months of age was observed, indicating long-lasting effects of early growth due to differential access to nutrients ($p < 0.05$ for female 24-month body weight, $p < 0.001$ for the rest; fig. S3, A and B). Furthermore, we observed an effect of litter size on longevity, apparently acting through body weight, as smaller litter size is associated with higher weight, which, in turn, is associated with shorter life span (*8*) (Fig. 2C). We therefore investigated whether including body weight and litter size as covariates in a longevity QTL scan would affect the results. Life span was remapped for males and females separately, without body weight, with body weight at 6 months (an age at which the relation is strongest), and with body weight at 6 months and litter size (fig. S3C). This analysis was performed for a total of 1122 control mice of both sexes, which resulted in similar linkages to the analysis excluding litter size as a covariate, albeit with reduced significance (highest peak in females is at chromosome 3 with empirical p value = 0.399). Logarithm of the odds (LOD) scores and significance are reduced by inclusion of body weight only in males. The inclusion of litter size in addition to body weight has little to no effect, in agreement with the mediation analysis in which the effect of litter size on longevity is mediated by body weight. Although the individual findings and pairwise relationships between litter size-growth and growth-longevity are not novel, here we provided an integrated view in a large and genetically heterogeneous mouse population.

We next asked if these relations are specific to UM-HET3 mice and whether we could establish similar associations in humans. We applied a Mendelian randomization (MR) strategy to large human datasets. Specifically, we assessed whether early and adult body size or height relate to parental longevity (a proxy of the individual's longevity) and indeed, early body weight at 10 years, height at 10 years, adult body mass index (BMI), but not adult height have potential negative effects on longevity (Fig. 2D) (*21*–*23*). An interesting finding is that the early body size effect is completely mediated by adult BMI (Fig. 2E). Height, by contrast, has a more complicated relationship with longevity, likely because it is also associated with higher socioeconomic status, which itself extends life span, and may be affected by population stratification (Fig. 2F) (*24*). Faster early growth may therefore be detrimental, but adult height may have antagonistic effects on longevity as it is jointly affected by growth and socioeconomic status.

To further deconstruct this, we performed an MR analysis for early and late height while excluding shared instrumental variables; that is, we used genetic instruments that are specific to each stage (Fig. 2G). Notably, the opposing effects become larger and more significant, supporting the hypothesis of distinct antagonistic age-specific effects of early and adult height on longevity. Finally, we analyzed whether the early height's effect is mediated by adult BMI in a manner similar to early weight through MR mediation and found that this is not the case, supporting a distinct relationship between early weight and height and longevity (Fig. 2H). An analogous investigation is not possible in our mouse population, as only body weight is available and not length or adiposity. Taken together, the interplay between different life-history traits that is similar between mice and humans shows that determinants of longevity can be decomposed into distinct genetic factors acting on other life-history traits, as well as nongenetic factors such as early growth, which may be controlled by early access and use of nutrients.

Analysis of body weight QTLs in relation to the longevity QTLs

Given the conserved age-dependent relationship between longevity and body weight across sexes and that this is also the case in humans, we explored whether variation in these traits is explained by the same genetic alleles. If that is the case, one explanation would be that the same genes may be universally affecting

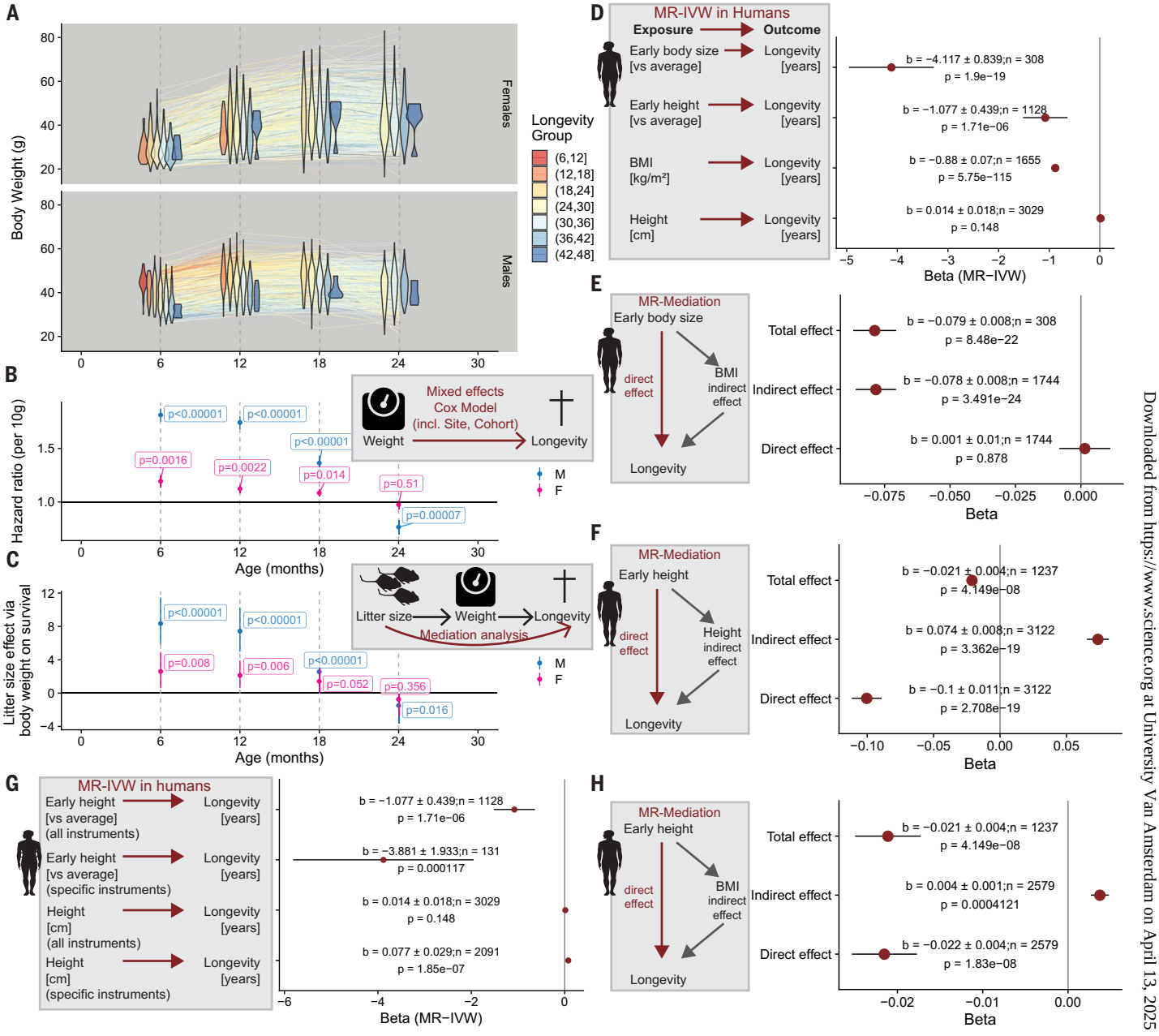

Fig. 2. Interplay between early growth, size, and longevity in mice and humans. (**A**) Inverse relationship between body weight and longevity is stronger in males than in females and at younger ages. Body weight trajectories of UM-HET3 mice, separated by sex. Each line represents body weight evolution of a single mouse. Body weight measurements were performed at 6, 12, 18, and 24 months, which are marked by vertical dashed gray lines. Mice are split into seven groups and colored on the basis of their longevity. Violin plots show the distribution of body weight at the measured ages. (**B**) Mixed-effects Cox model hazard ratio of an increase in 10 g in body weight in males and females, as well as the 95% confidence interval and *p* value (*8*). (**C**) Effect of litter size on survival mediated by body weight at different ages using mediation analysis (b indicates effect size, and n is the number of instruments). (**D**) Inverse variance weighted Mendelian randomization results for body weight and height and parental life span (*22*). Early body size and heights are the comparative body weight and heights at age 10 of ~500,000 individuals from the UK Biobank (data fields 1687 and 1697, respectively). BMI (body mass index) is from ~700,000 individuals (*23*). (**E**) MR-Mediation analysis shows that the effect of early body weight is completely mediated by BMI. (**F**) MR-Mediation shows that the effect of early height is not mediated by height. (**G**) Because adult and early height share genetic associations (or instrumental variables, IVs), MR was performed with the IVs that are specific to each phenotype, excluding the common IVs, further enhancing the opposing effects of early and adult height. (**H**) MR-Mediation shows that the effect of early height is not mediated by BMI.

different facets of aging, for which body weight and longevity act as surrogate traits. For that, we performed QTL mapping in the UM-HET3 mice with a total of four models, as we had done for longevity (Fig. 3A, and fig. S4A).

We detected sex-specific body weight QTLs that are conserved at different ages. For instance, we identified a female body weight QTL at chromosome 7 at all ages, and one at chromosome 6 that is significant until 18 months ($p < 0.05$). Some other QTLs were also conserved in at least two different ages such as those on chromosomes 5,6, and 15 in females and 9 and 17 in males. Indeed, a previous QTL study in UM-HET3 combining two sexes had already

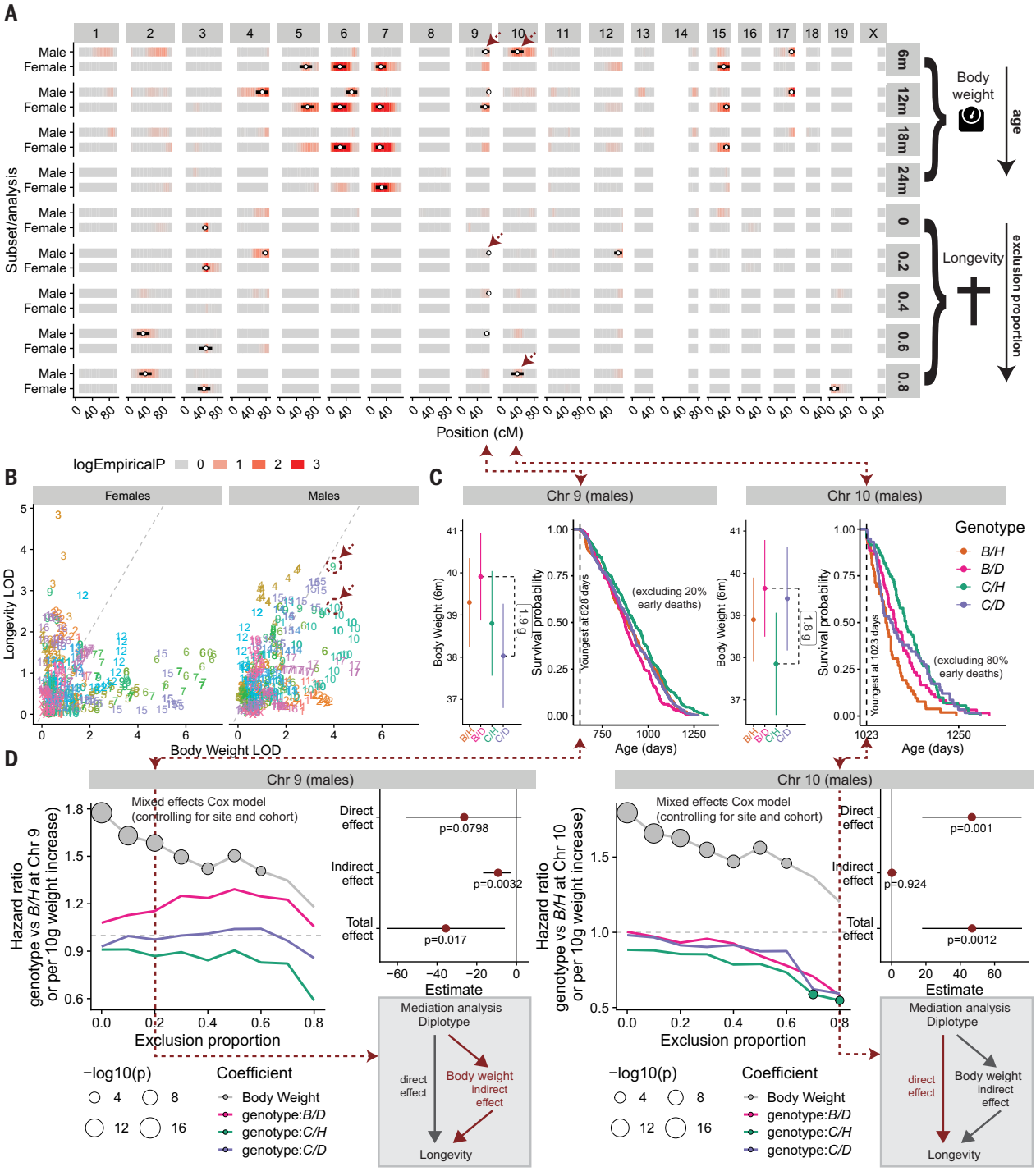

Fig. 3. QTL mapping of body weight identifies sex-specific loci and evidence of shared genetic effects on longevity in males. (**A**) QTL mapping results for sex-specific body weight at different ages and longevity scans at different exclusion levels. Each locus is colored by the −log10(empirical *p* value), and QTL peaks are marked with a black line [see (*8*) for peak definition]. The peak location of each locus is marked by a white dot. Red arrows mark the two loci on chromosomes 9 and 10 where QTL signals for longevity and body weight colocalize. (**B**) Scatterplot of the LOD scores at each marker for longevity and body weight at 6 months on the vertical and horizontal axes, respectively. Each marker is labeled and colored by the chromosome on which it resides. Circles show the markers that were further examined in (C) and (D). (**C**) Effect plots for body weight at 6 months by genotype, as well as survival curves, at the chromosome 9 and 10 loci in males (excluding 20 and 80% of early deaths, respectively). In the effect plot, the mean body weight and standard deviations per genotype are represented, as well as the difference between the highest and lowest averages. The dashed red lines are visual aids to connect the longevity and body weight QTL colocalizations in (A) and the allelic effects in (C). (**D**) Mixed-effects Cox model of the association of genotype and body weight as a function of different truncation proportions (nine truncation levels from 0 to 0.8). Points are drawn when the *p* value is less than the Bonferroni-corrected *p*-value threshold (0.05/9 = 0.0056). B/H is the reference genotype to which all others are compared. The mediation analysis is performed at the indicated truncation levels (0.2 and 0.8 for chromosome 9 and 10 loci, respectively) to match the longevity association results.

identified the loci on chromosomes 6, 7, and 15 (*14*) that also agree with the findings here in terms of directionality and magnitude (Fig. 3B). Notably, these earlier results were performed in one site, whereas the current data are from two sites across many years. With the exception of a locus on distal chromosome 9 for male and female body weight, which also overlaps with the male longevity QTL, there were no instances of the same QTL emerging in both sexes (fig. S4A), indicating that the genetic effects on body weight are predominantly sex specific. In sex-combined QTL scans, some QTLs overlap with existing sex-specific QTLs (chromosomes 10 and 17 for males and 5, 6, 7, and 15 for females), and some additional QTLs are evident on chromosomes 2 and 11. In terms of sex-by-genotype interaction, we identified loci on chromosomes 7 and 15. We also performed QTL scans for body weight change that yielded a single QTL on chromosomes 4 in males and 5, 6, and 7 in females, overlapping with body weight QTLs (fig. S4A). These results do not support the presence of genetic modifiers of rates of body weight changes in adult mice that are distinct from the determinants of body weight.

Although we identified significant QTLs in most analyses, this ensemble of QTL mapping results for longevity, body weight, and body weight change suggests that there is little QTL sharing across sexes and traits (Fig. 3A; fig. S4, A and B; and data S2 and S3). There are no overlaps in females, whereas in males, the chromosome 4 and 9 loci and the age- and male-specific longevity locus at chromosome 10 overlap with body weight loci. Indeed, when we observed the genome-wide relationship between the LOD scores for longevity and body weight QTL scans, we saw that they correlate in males but not in females, paralleling the strong relationship at the phenotypic level (Pearson correlation in males = 0.339, $p = 2.33 \times 10^{-12}$, Fig. 3B). The male-specific colocalization may either be the result of the two traits' correlation or due to genetic effects on longevity being mediated by genetic regulation of body weight. To distinguish between these two possibilities, we examined the effect of each genotype on longevity and body weight and performed mediation analyses.

We found no relationship between the genetic association with body weight and longevity on chromosome 4 (fig. S4C). That is, mice carrying the lightest allele are not the longest-lived or vice versa. This is an indication that body weight modulation and longevity are distinctly affected by genetic variants in this locus. By contrast, male mice with the *B/D* combination on the distal chromosome 9 locus are the heaviest at 6 months and the shortest-lived (Fig. 3C). Similarly, mice carrying the *C/H* at the chromosome 10 longevity locus (when 80% of deaths are excluded) are the lightest at 6 months and the most long-lived (Fig. 3C). These patterns chromosomes 9 and 10 raise the possibility that the effect of genetic variation on longevity is through modulation of body weight or growth.

To further examine these two loci, we tested whether including body weight in a Cox model would extinguish the genetic effect we observe on longevity (Fig. 3D). For chromosome 9, we observed that body weight, and not genotype, is significantly associated with hazard ($p = 6.15 \times 10^{-11}$). In addition, a mediation analysis illustrates that the effect of genotype on longevity is predominantly mediated by body weight. The chromosome 10 male locus, however, shows signs that the genetic effect on longevity is independent on the effect on body weight. The *C/H* genotype combination is significantly associated with male longevity when at least 70% of early deaths are removed even when controlling for body weight ($p = 0.0021$). In addition, the mediation analysis shows that the effect of genotype is direct and not through body weight. Taken together, these results designate the loci on chromosomes 4 and 10 as male-specific longevity modifiers through an unknown mechanism, whereas a locus on chromosome 9 may be modulating longevity through its effect on growth or body weight.

Liver gene expression reveals age- and sex-related differences in gene- and haplotype-specific expression

Having identified several QTLs for longevity and body weight, we next explored the genes under the QTL peaks in an effort to shortlist candidate longevity genes. Because the identified QTLs are large owing to limited recombination in a four-way intercross, there may be dozens of genes under each QTL. Furthermore, genetic variation within or around these genes may affect the gene's function either directly or through regulatory variation (*25*). We devised multiple strategies to home in on candidate causal genes within these loci, none of which provides enough confidence in isolation. For instance, endophenotypes such as gene expression allow a more fine-grained investigation of genetic effects on quantitative traits and typically have a simpler genetic architecture. We performed RNA sequencing (RNA-seq) of 33 livers from adult (6 month) and old (22 month), male and female UM-HET3 mice to identify genes with allele- and haplotype-specific expression (HSE).

Prior to HSE analysis, we characterized the effects of sex and age by performing differential gene expression for age, sex, and age-by-sex interaction, followed by gene set enrichment analysis (*8*) (fig. S5A and data S4). Although most of these age-related changes in gene expression are not expected to be causal (*26*), they provide insights into the footprint of aging (*27*, *28*). Differential expression in livers of UM-HET3 mice has already uncovered genes whose expression is related to life span–extending interventions (*29*). However, it is not clear if differentially expressed genes are more likely to explain interindividual differences in aging or longevity than genes whose expression remains stable with age. There were 444 sex- and 190 age-related differentially expressed genes (absolute $\log_2$ fold change > 1, BH-adjusted $p < 0.05$). The most significant functional enrichment for the sex effect is in the "cellular response to interferon-β" gene ontology term, with genes expressed higher in females (adjusted $p = 0.047$; Fig. 4, A and B). The interferon response is not only sexually dimorphic and higher in female mice (*30*) but also a major determinant in mediating severity of infections, including COVID-19, likely explaining higher mortality in men who have lower type I interferon activity than women (*31*, *32*). It is therefore possible that differences in interferon response may play a contributing role in the sex- and age-specific differences in disease susceptibility.

As for the effect of age on liver expression, we observed very significant enrichment of immune-related terms in genes whose expression increases with age (adjusted $p < 0.05$) and no significant enrichment in those with decreased expression (Fig. 4A). This is in line with previous findings that there are more genes that are consistently expressed with age than are underexpressed and that the overexpressed genes tend to be immune related (*33*). Specifically, the most enriched biological processes relate to leukocyte activation and proliferation, possibly reflecting a change in tissue composition due to increased number or activity of infiltrating or resident immune cells in the aged liver. Indeed, published single-cell RNAseq data indicate that changes in liver cellular composition, as well as an increase in immune signature, occur with age (*34*). Specifically, the relative number of hepatocytes decreases, whereas the number of liver sinusoidal endothelial cells (LSECs) increases. By contrast, Kupffer cells seem to remain stable in numbers, but more of them express *Il1b* in older mice. To corroborate these findings, we performed single-cell deconvolution analysis on the bulk RNA-seq results (*8*) (Fig. 4C). We detected changes in estimated cell type proportions only in males, with significant loss in hepatocyte number (Dirichlet regression p value = 0.00024) and gain in B cells, Kupffer cells, and LSECs ($p = 0.011, 0.013, 9 \times 10^{-4}$, respectively), in line with single-cell analyses (*34*). Taken together, the age-related changes in gene expression in UM-HET3 livers support established functional and compositional changes, an indication of the conservation of major age-related changes across studies.

We also exploited the presence of segregating UM-HET3 variants to detect HSE (*8*) (Fig. 4, D and E; fig. S5, B to E; and data S5). Allelic imbalance is a pervasive phenomenon

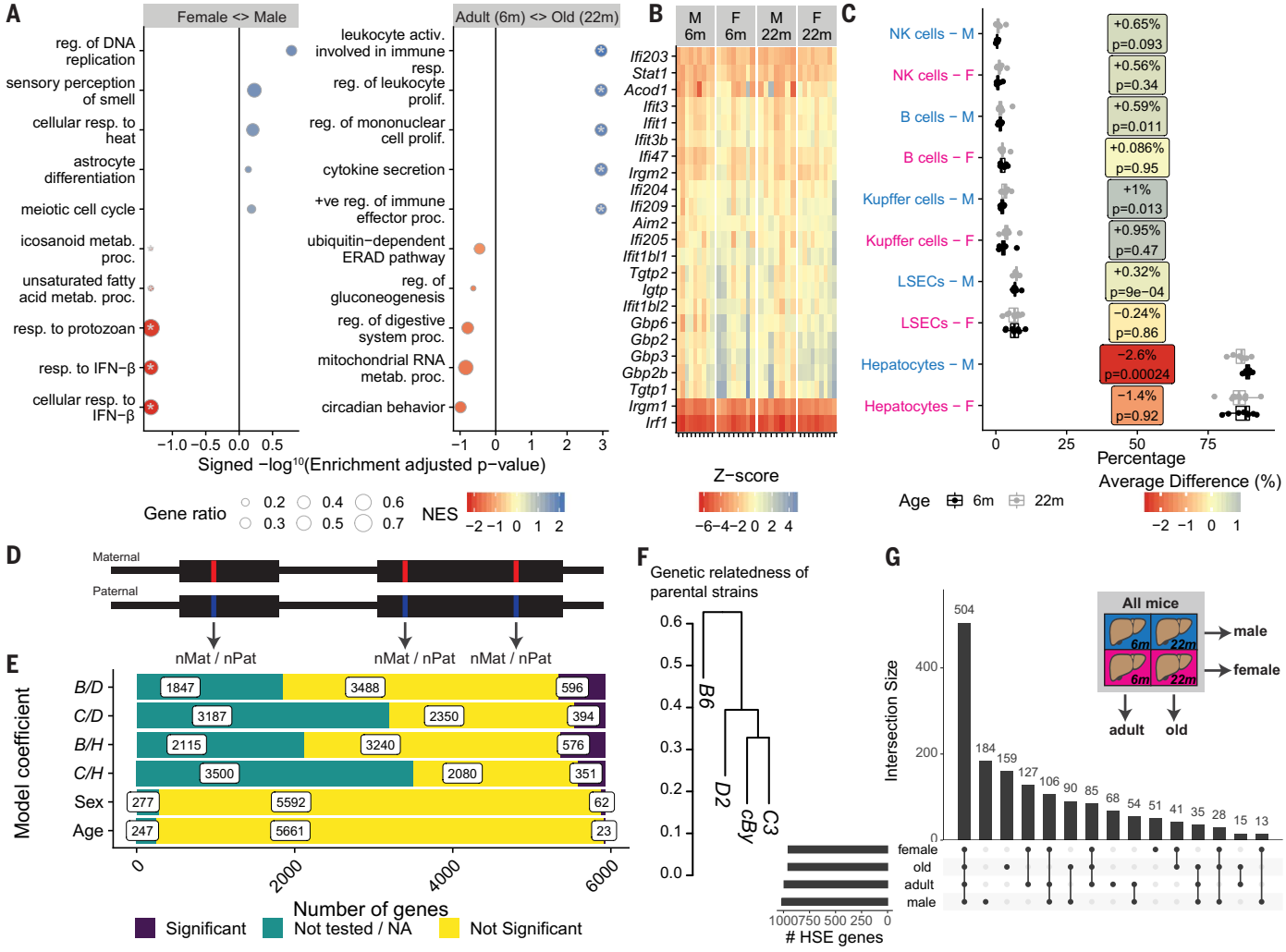

Fig. 4. Liver gene expression reveals age- and sex-related differences in gene and haplotype-specific expression. (**A**) Gene set enrichment analysis of biological processes in sex- and age-related differences in UM-HET3 liver gene expression. A positive value indicates an enrichment of a gene set driven by higher expression of its genes in males (in the left panel) or an expression increase due to age (in the right panel). (**B**) Heatmap illustrating the expression levels of genes contributing to the enrichment of cellular response to IFN-β in females when compared to males. (**C**) Cell type proportions as estimated using single-cell deconvolution analysis. NK, natural killer; LSECs, liver sinusoidal endothelial cells. For each cell type and sex, the mean difference in cell proportions is represented along with the *p* values for the age group effect from Dirichlet regression was applied to each sex separately. (**D**) Workflow and results of haplotype-specific expression (HSE) analysis. Each mouse was first genotyped at every polymorphic locus, then haplotype calling was performed. The numbers of maternal and paternal reads were collected and used in several binomial generalized linear mixed models to test for the effect of haplotype, age, and sex. (**E**) HSE results for the whole dataset. Within each model, genes were divided into whether the parameter's *p* value is significant (at a BH-adjusted $p < 0.05$). "Not tested / NA" indicates that coefficients could not be estimated for a model component for a certain gene. Stacked bar plots indicate the number of genes in each group. Text labels are the number of genes. (**F**) Hierarchical clustering of genetic relatedness of parental strains explains differences in the number of detected HSE genes per genotype. The more distant the strain pair, the more HSE genes are detected (*8*). (**G**) UpSet plot of the number and sharing of genes with significant HSE across different analysis subsets.

in mice that is affected by parent-of-origin effects and regulatory variation, which contributes to complex traits (*35*–*37*). The main rationale is that an allelic imbalance under a QTL of a complex trait may be causal and underlying variation in longevity or body weight. The fact that allele-specific expression is directly implicated in disease or useful in inferring causal mechanism of disease-associated loci provides further support to this approach (*38*). Briefly, we inferred genotypes on the basis of the RNA-seq data and used a binomial generalized linear mixed model to infer whether sex, age, or specific haplotype combinations affect the ratio of maternal to paternal transcripts or allelic imbalance. The data and specific experimental design allowed us to assess HSE in ~6000 genes, using ~70,000 variants (Fig. 4E). Using this strategy, we attributed the measured bias in maternal to paternal reads to age, sex, or one of the genotypes. For example, there are 23 and 62 genes for which a bias in expression can be attributed to sex and age, respectively. As expected, identified HSE is mostly attributed to genotype effects, with *B/D* having the most and *C/H* the fewest HSE events (596 and 351 significant, respectively). It is noteworthy that the UM-HET3 parental strains are not genetically equidistant from each other, with B6 being the most distant from the three other

strains and C3 and cBy being the closest pair (Fig. 4F). This genetic relatedness, coupled with the cross design, implies that some haplotype combinations are more likely to have HSE than others, simply because of differences in the abundance of variants enabling HSE inference (Fig. 4, E and F). Specifically, it is more likely to detect HSE in genes in mice that are carrying the *B* maternal allele, as the B6 strain is genetically the most distant from the three other strains.

We compared the results of HSE separately on different subsets (males of both ages, females of both ages, young adults of both sexes, old of both sexes) by finding overlaps of genes with HSE (Fig. 4G). The largest set of genes (n = 504) is the intersection of all subsets and consists of genes that have HSE independent of sex or age, likely ones with robust determinants in cis. The next largest set (n = 184) is male specific, followed by one that is specific to old mice (male and female), suggesting that some of the observed HSE effects may be mediated by sex- or age-specific factors.

Cross-species search of candidate genes implicated in longevity modulation

Having identified QTLs for body weight and longevity, gene expression differences by sex and age, and HSE for different ages and sexes, we combined all this information to catalog and develop a simple scoring scheme for genes under QTLs (*8*) (table S2, Fig. 5, and data S6). Because genetic variation can affect a protein-coding gene's function, we examined whether genes have high-impact variants (HIVs) that may affect their splicing or coding potential in one of the parental strains. We further determined whether these variants segregate in the UM-HET3 in a way that is consistent with the observed QTL effect. We postulated that genes under the QTL with age-related differential expression (DE) could be of interest in hypothesis building, even if DE may be a result and not a cause of aging, so we investigated whether the gene is differentially expressed in the liver dataset. Finally, to detect regulatory variant effects on gene expression, which could be driving the QTL signal, we asked whether the genes exhibit HSE.

Going beyond UM-HET3, we expanded the search toward other mouse and model organism databases. We examined whether QTL genes are differentially expressed in all the tissues of Tabula Muris Senis (TMS) (*34*) and gave an additional point if they are differentially expressed in multiple tissues. In addition, we extended the search to model organisms and cross-referenced the genes and their orthologs with the GenAge database, which contains a curated list of longevity genes (*39*). Additional points were given if a gene is a known longevity gene in mice or in more than one species.

In addition to analysis of mouse data, we also characterized the genes' human orthologs by mirroring the available mouse data generated in this study that span the genetic, gene expression, and genetically driven gene expression (*8*). First, we checked for age-associated DE in all GTEx tissues (*40*). Additional points were given if the gene is differentially expressed in more than one tissue. Then we looked at whether there is any human genome-wide association study (GWAS) hit for longevity (or BMI for the mouse body weight QTLs). To establish genetic links between gene expression and BMI and longevity, we performed transcriptome-wide Mendelian randomization (TWMR) (*41*). The combination of all these data serves as a hypothesis-building knowledge base for longevity and body weight genes. Figure 5B shows genes with a minimum score of 5 under the longevity QTLs of females, and males with 20% and males with 80% truncation, representing early and late determinants of male longevity (data S6 includes all the annotations and scores). Although the results of this investigation cannot attribute causal roles to these genes in longevity modulation, they provide valuable candidates for in-depth mechanistic studies that capitalize on our system's genetics observations. We illustrate this by performing survival analyses in *C. elegans* to test whether RNA interference (RNAi)–knockdown of the worm orthologs of the top-scoring genes would modulate longevity, therefore highlighting interesting genes for follow-up (Fig. 5C and fig. S6).

In the female longevity locus on chromosome 3, the five highest-scoring genes are *Ctss*, *Ecm1*, *Fcrl1*, *Hipk1*, and *Etv3* (aggregate score ≥ 5; Fig. 5B and data S6). Among those, we could validate the orthologs of *Ctss* (*K02E7.10* and *Y113G7B.15*) and *Hipk1* (*hpk-1*) in the worm and find that *hpk-1* RNAi significantly reduces life span (p < 0.0001; Fig. 5C and fig. S6). Indeed, *hpk-1* is already annotated as a worm pro-longevity gene in GenAge (*42*), and the transcriptional cofactor that it encodes has been shown to maintain proteostasis and extend longevity (*43*). The *ETS Variant Transcription Factor 3* (*Etv3),* which has an HIV with segregation patterns concordant with longevity and is differentially expressed in UM-HET3 and in TMS, has not been implicated in mammalian aging. However, the *Drosophila* ETS family members, *Aop* and *Pnt*, have been found to control longevity (*44*). Similarly, *Ctss* has HIV, HSE, and is differentially expressed in multiple TMS tissues, yet has not been implicated in mammalian aging. More in-depth studies would be required to assess the roles of the top-scoring genes.

For the early male longevity QTLs excluding 20% of deaths, the top-scoring genes are *Alpl*, *Eif4g3*, *Ece1*, *Pafah2*, *Hspg2*, and *Ddost* (aggregate score > 5; Fig. 5B and data S6). The highest-scoring gene is the tissue-nonspecific or liver, bone, kidney-type alkaline phosphatase (*Alpl*) gene that also harbors an HIV, exhibits HSE but has a decreasing expression in the UM-HET3 liver, and is differentially expressed in GTEx adipose tissue. More investigation is required to confirm this gene and establish a mechanistic link with longevity. We tested orthologs of all genes except *Alpl*, which does not have a worm ortholog, and found that *unc-52* (*Hspg2*) and *ostb-1* (*Ddost*) RNAi both significantly shorten life span (p < 0.0001; Fig. 5C and Fig. S6). Although *unc-52* is already known to affect worm life span (*45*, *46*), *ostb-1* or its ortholog (*Ddost*) has not yet been directly linked to longevity. However, Dolichyl-diphosphooligosaccharide–protein glycosyltransferase noncatalytic subunit (DDOST) is implicated in processing advanced glycation end products (AGEs) (*47*), which accumulate with age and exacerbate the aging phenotype (*48*). In the UM-HET3, the gene has HIVs as well as HSE, which may affect rates of AGE processing and ultimately longevity.

In the late male longevity QTLs excluding 80% of deaths, 11 genes have an equal aggregate score of 5: *Ank3*, *Slc25a3*, *Vezt*, *Stab2*, *Gnptab*, *Tdg*, *Fgd6*, *Slc17a8*, *Abcb11*, *Slc25a12*, and *Pdk1* (Fig. 5B and data S6). We tested the orthologs of *Ank3*, *Slc25a3*, *Fgd6*, *Slc17a8*, *Abcb11*, *Slc25a12*, and *Pdk1* in *C. elegans* (Fig. 5C and fig. S6). Of those, *tag-77* (*Fgd6*) and *pdhk-2* (*Pdk1*) shortened and increased life span, respectively (p = 0.0019 and p < 0.0001). Whereas the *tag-77* RNAi life-span reduction is modest compared with the other significant RNAi effects (~14% reduction in median and maximum life span), a locus near human *FGD6* (rs12830425) has been recently found to be associated with health span, life span, and exceptional longevity, rendering it a very interesting cross-species aging and longevity candidate gene (*49*). Pyruvate dehydrogenase kinase 1 (Pdk1) regulates cellular energetics, as its kinase activity inactivates pyruvate dehydrogenase (PDH) activity, thereby shutting down glucose oxidation in the mitochondrion. In agreement with our results, RNAi and mutations in *pdhk-2* have been previously shown to extend worm life span (*50*). As PDH complex has been proposed to be a therapeutic target for age-related diseases, Pdk1 modulation may be appealing as an anti-aging intervention because it is a known target of dichloroacetate (*51*). Some of the top-scoring late male longevity QTL genes encode mitochondrial proteins (*Slc25a3*, *Slc25a12*, *Pdk1*). Mitochondrial dysfunction has been extensively linked to growth and longevity regulation in model organisms (*52*–*54*). In addition to their metabolic role, mitochondria affect other features of aging such as epigenetics and proteostasis, hence acting as a central hub in the aging process (*4*, *5*). As a case in point, mitochondrial health is associated with a 31%

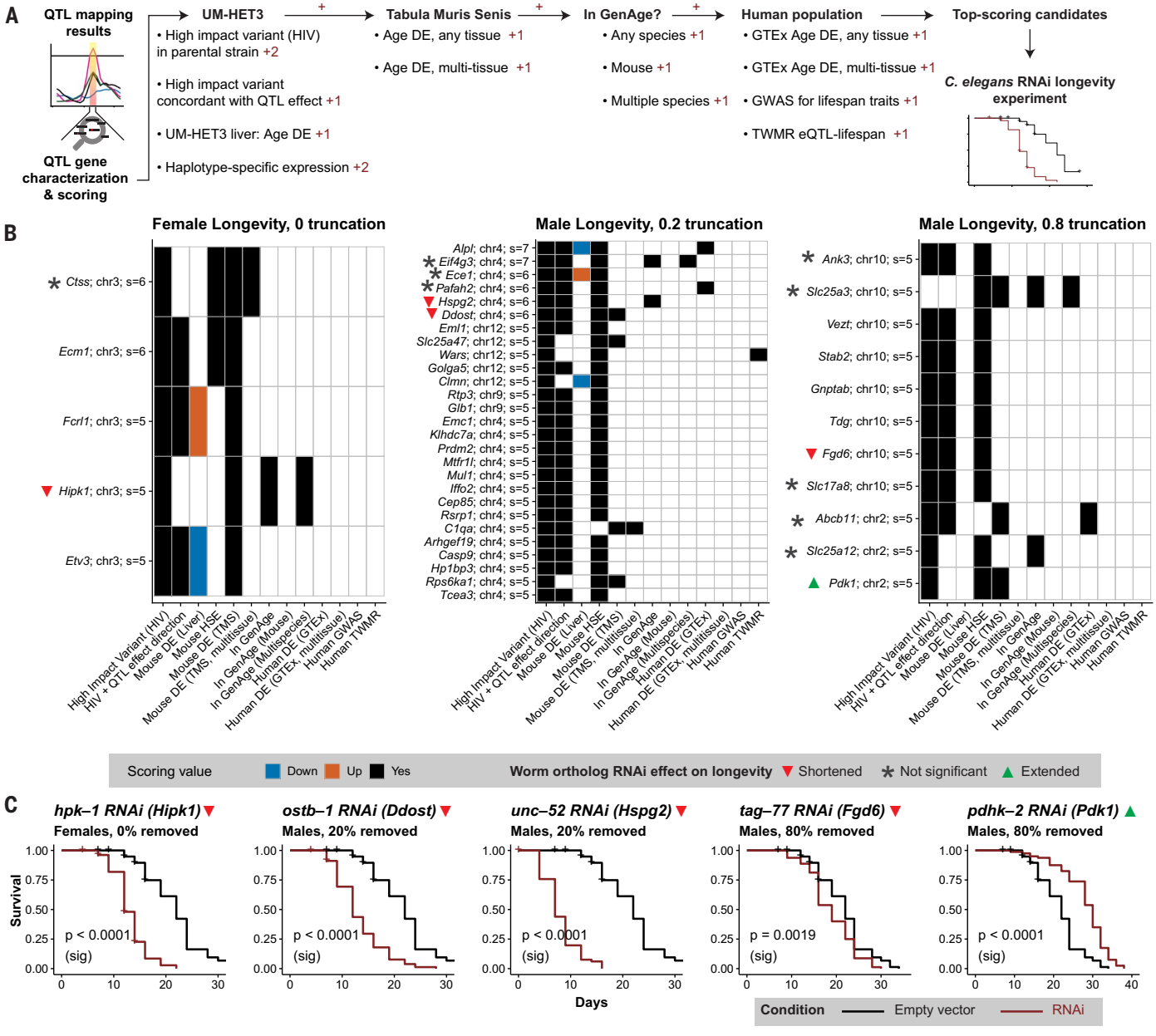

Fig. 5. Annotation, prioritization, and validation of candidate longevity genes. (**A**) Diagram of the gene annotation and scoring pipeline. Scores are indicated in red. Genes under longevity QTL peaks were annotated based on whether they (i) have a high impact variant (HIV) in one of the UM-HET3 parents; (ii) have an HIV whose parental alleles are in line with the direction of the QTL's effect; (iii) are differentially expressed in the UM-HET3 livers; (iv) show haplotype-specific expression in UM-HET3 livers; (v) are differentially expressed in any tissue in the *Tabula Muris Senis* (TMS); (vi) are differentially expressed in more than one TMS tissue; (vii) are or have orthologs that are already in GenAge; (viii) are in GenAge in the mouse; (ix) are in GenAge in multiple species; (x) have a differentially expressed human ortholog in any GTEx tissue; (xi) are differentially expressed in GTEx in multiple tissues; (xii) have been identified in human GWAS for longevity or age-related disease; or (xiii) have a link to longevity through transcriptome-wide Mendelian randomization (TWMR) (*41*). Genes that have a worm ortholog and an available RNAi clone were further validated and marked based on whether there is shortened, extended, or unchanged life span. (**B**) Top-scoring genes under selected longevity QTL genes. (**C**) Significant effects of RNAi-mediated knockdown of worm orthologs of some of the highest-scoring genes. Eighty worms were used per group and the log-rank test was performed. Worms that escaped from the plates or had vulva explosions were censored from the life span measurements. Nominal *p* values are indicated and significance is determined after Bonferroni correction (n = 19 genes tested in total; see fig. S6 for all tested genes).

longer life span in rats selectively bred for higher intrinsic exercise capacity (*55*). It is worth noting, however, that the late male longevity locus on chromosome 10 also contains genes known to affect aging such as *Igf1*, *Sirt1*, and *Sirt6*, yet these genes have not been prioritized on the basis of criteria used in this study (data S6).

As the results here serve for hypothesis generation rather than to establish causal relations, they provide a resource for the community. For that purpose, we developed an interactive web application that is helpful to explore the entirety of the results (https://www.systems-genetics.org/itp-longevity).

Discussion

Our analyses draw a general picture in which the effects of genetic factors are mostly sex, age, and trait specific. One key finding is that many of the QTLs seem to modulate life span only in mice beyond a certain age, especially in males. We find that genetic determinants of longevity and body weight variation are different and sex specific even though the two traits are highly correlated. These two traits are more correlated in males, leading to some overlaps in the identified QTL peaks. Using mediation analysis, we could discern whether overlaps in male-specific longevity and body weight QTL are due to distinct genetic effects on each trait (chromosomes 4 and 10) or genetic effects on body weight affecting longevity (chromosome 9).

Although our work did not document a large number of segregating loci with detectably large effects on life span in both male and female mice, it is possible that life span is instead modulated by a large number of loci with smaller individual effects. It is also possible that life span is modulated by interactions among segregating loci (gene-by-gene interactions). Regulation of insulin-like growth factor 1 (IGF1) levels in UM-HET3 mice, for example, has been shown to be influenced largely by three-gene and four-gene combinations (*56*), so that extreme levels of IGF1 require allele combinations present in only 1/8 or 1/16 of the population. Our methods do not consider gene-by-gene interactions of this kind and may have missed life span loci that have effects only in specific genetic contexts.

The combination of high heterozygosity in any single mouse combined with variability across mice means that the UM-HET3 are more heterogeneous than most mice currently used in research, most of which are inbred. However, we note that all four inbred grandparents of the UM-HET3 population have undergone hundreds of generations of selection for breeding success in laboratory conditions and may well have lost genetic variants, present in natural mouse populations, with major effects on maturation rate, growth rate, body size, IGF1 levels, and life span. There is evidence, for example, that offspring of crosses between wild-trapped mice and laboratory-adapted stocks of mice vary in IGF1 levels, with high life span associated with lower IGF1 levels within these segregating F_2 populations (*57*). Restricting our genetic analysis to alleles present in laboratory-adapted stocks would prevent us from detecting alleles present only in wild mouse populations.

It is also plausible that segregating alleles that do influence life span in UM-HET3 mice are principally effective in one but not both sexes. Genetic analysis of *Drosophila* longevity (*58*) has shown that most life-span loci are indeed sex specific, and studies of drugs that modulate mouse life span have also shown sex specificity for more than half of the effective drugs (*59*–*61*). The apparent near-absence of loci with strong, sex-independent effects on life span does not preclude the possibility that shared processes—such as proteostasis, mitochondrial protection, inflammation, stress-resistance pathways, and many others—could contribute to regulation of aging and longevity in both sexes.

In addition to genetics, nongenetic factors such as very early growth and access to nutrients play a role in determining longevity. Although the relationship between early growth, metabolism, and growth has been established through direct experimentation (*14*, *62*), it is important to shed light on these effects in the ITP UM-HET3 mice. Understanding how genetics affects longevity will thus inevitably require accounting for the different effects of genetics, life history, and environment on processes that affect aging, disease risk, and mortality. Indeed, we show that litter size has a negative association with body weight and a marked indirect effect on longevity.

Not all aspects of mouse physiology are expected to be identical in humans, as has been shown in a study showing that, in contrast to humans, mouse fasting glucose levels increase with age and higher glucose is associated with longer life span (*63*). In the same study, however, the longitudinal trajectories of body weight and fat were shown to be similar between mice and humans. Therefore, there may be sufficient similarities for genetic studies in mouse populations to inform studies on human aging. Here we show that relationships between early growth, body size, and longevity are also conserved in humans. Specifically, the MR and MR-mediation analysis of the UK Biobank data indicate that early growth is likely causal in determining adult longevity, through its effect on adult BMI. BMI is determined by adiposity and size in different ways than body weight in mice; hence exploring similarities between mice and humans will require measurements of body composition and size in mice, data which are not available in the ITP.

In terms of gene expression, the liver profiles reveal a strong increase in immune-related transcripts with age, which is indicative of chronic inflammation or inflammaging (*64*). Another case in point is that females, who are longer-lived than males, have a higher expression of interferon-β (IFN-β)–related genes, consistent with previous observations (*30*). This is reminiscent of the situation in humans where the more vigorous IFN-β response in women has been invoked to explain the attenuated severity of infections, including COVID-19, likely explaining higher mortality in males (*31*). It is therefore possible that differences in interferon response gene activity may play a contributing role in the sex- and age-specific differences in disease susceptibility. We capitalized further on the fact that UM-HET3 mice are heterozygous to detect extensive haplotype-specific expression across two sexes and two ages. This information was used to help prioritize genes under QTL peaks and could also serve as a resource for more in-depth study of the effect of regulatory variation on gene expression.

The characterization of genes under QTLs provides a resource for further investigation of their putative roles in mediating longevity and body weight variation (see interactive application: https://www.systems-genetics.org/itp-longevity). Future studies that include more ITP mice as well as denser genetic maps may yield improved QTL results. Finally, more longitudinal data collection accompanied by extensive phenotyping would be required to shift the focus from longevity to a better understanding of genetics of healthy aging or health span. There is therefore great potential to reach valuable insights into aging by feeding into the virtuous cycle between mouse genetics and human drug discovery, which has already been a successful paradigm in identifying disease genes for drug discovery (*65*).

Materials and methods summary

Phenotype and genotype data of UM-HET3 mice from the ITP

The UM-HET3 mice are genetically heterogeneous progeny of CByB6F1 females and C3D2F1 males, produced at each of three sites—the Jackson Laboratory (JL), the University of Michigan at Ann Arbor (UM), and the University of Texas Health Science Center at San Antonio (UT) (*6*). Experiments at the JL, the UM, and the UT were reviewed and approved annually by the Institutional Animal Care and Use Committees at each site. Life span and weight data for ITP mice were compiled by the laboratories of D. Harrison, R. Miller, and R. Strong, and are available in the Mouse Phenome Database (*66*). Litter size data were provided by J. Nelson. Tail samples were sent to GeneSeek (Neogen Corporation), where genomic DNA was extracted, followed by single-nucleotide polymorphism (SNP) genotyping by matrix-assisted laser desorption/ionization–time-of-flight mass spectrometry (*67*) at a maximum of 270 markers.

QTL mapping

Longevity

To assess the effect of haplotype on longevity, we used the coxme package to fit multiple mixed-effects Cox models. The full model includes the two sexes and has sex as a fixed effect and site as a random effect. The cohort year was included as a random effect that is nested in site. The sex-specific models do not have sex as a fixed effect. To define significance thresholds, we performed 1000 permutations with label swapping. We systematically performed

QTL mapping for longevity by eliminating different percentiles (or quantiles) of the shortest-lived mice.

Body weight

We employed a similar strategy as for longevity but using the lme4 package to fit mixed linear models.

Web application

We developed an application using the R Shiny package to allow researchers to browse the raw data and results of this project: https://www.systems-genetics.org/itp-longevity.

Full materials and methods are available in the supplementary materials (*8*).

REFERENCES AND NOTES

1. C. López-Otín, M. A. Blasco, L. Partridge, M. Serrano, G. Kroemer, The hallmarks of aging. *Cell* **153**, 1194–1217 (2013). doi: 10.1016/j.cell.2013.05.039; pmid: 23746838
2. C. J. Kenyon, The genetics of ageing. *Nature* **464**, 504–512 (2010). doi: 10.1038/nature08980; pmid: 20336132
3. M. Hook *et al*., Genetic cartography of longevity in humans and mice: Current landscape and horizons. *Biochim. Biophys. Acta Mol. Basis Dis.* **1864** (9 Pt A), 2718–2732 (2018). doi: 10.1016/j.bbadis.2018.01.026; pmid: 29410319
4. L. N. Booth, A. Brunet, The aging epigenome. *Mol. Cell* **62**, 728–744 (2016). doi: 10.1016/j.molcel.2016.05.013; pmid: 27259204
5. R. C. Taylor, A. Dillin, Aging as an event of proteostasis collapse. *Cold Spring Harb. Perspect. Biol.* **3**, a004440 (2011). doi: 10.1101/cshperspect.a004440; pmid: 21441594
6. R. A. Miller *et al*., An Aging Interventions Testing Program: Study design and interim report. *Aging Cell* **6**, 565–575 (2007). doi: 10.1111/j.1474-9726.2007.00311.x; pmid: 17578509
7. N. L. Nadon *et al*., Design of aging intervention studies: The NIA interventions testing program. *Age (Dordr.)* **30**, 187–199 (2008). doi: 10.1007/s11357-008-9048-1; pmid: 19424842
8. See supplementary materials.
9. F. Macchiarini, R. A. Miller, R. Strong, N. Rosenthal, D. E. Harrison, "Chapter 10 - NIA Interventions Testing Program: A collaborative approach for investigating interventions to promote healthy aging" in *Handbook of the Biology of Aging (Ninth Edition)*, N. Musi, P. J. Hornsby, Eds. (Academic Press, 2021; https://www.sciencedirect.com/science/article/pii/B978012815962000010X), *Handbooks of Aging*, pp. 219–235.
10. C. J. Cheng, J. A. L. Gelfond, R. Strong, J. F. Nelson, Genetically heterogeneous mice exhibit a female survival advantage that is age- and site-specific: Results from a large multi-site study. *Aging Cell* **18**, e12905 (2019). doi: 10.1111/acel.12905; pmid: 30801953
11. A. U. Jackson, A. T. Galecki, D. T. Burke, R. A. Miller, Mouse loci associated with life span exhibit sex-specific and epistatic effects. *J. Gerontol. A Biol. Sci. Med. Sci.* **57**, B9–B15 (2002). doi: 10.1093/gerona/57.1.B9; pmid: 11773201
12. R. Gelman, A. Watson, R. Bronson, E. Yunis, Murine chromosomal regions correlated with longevity. *Genetics* **118**, 693–704 (1988). doi: 10.1093/genetics/118.4.693; pmid: 3163317
13. C. J. Bult *et al*., Mouse Genome Database (MGD) 2019. *Nucleic Acids Res.* **47**, D801–D806 (2019). doi: 10.1093/nar/gky1056; pmid: 30407599
14. R. A. Miller, J. M. Harper, A. Galecki, D. T. Burke, Big mice die young: Early life body weight predicts longevity in genetically heterogeneous mice. *Aging Cell* **1**, 22–29 (2002). doi: 10.1046/j.1474-9728.2002.00006.x; pmid: 12882350
15. S. Roy *et al*., Gene-by-environment modulation of lifespan and weight gain in the murine BXD family. *Nat. Metab.* **3**, 1217–1227 (2021). doi: 10.1038/s42255-021-00449-w; pmid: 34552269
16. W. H. Dietz, Childhood weight affects adult morbidity and mortality. *J. Nutr.* **128** (Suppl), 411S–414S (1998). doi: 10.1093/jn/128.2.411S; pmid: 9478038
17. C. Maffeis, L. Tatò, Long-term effects of childhood obesity on morbidity and mortality. *Horm. Res.* **55** (Suppl 1), 42–45 (2001). pmid: 11408761
18. M. E. Bowen, The relationship between body weight, frailty, and the disablement process. *J. Gerontol. B Psychol. Sci. Soc. Sci.* **67**, 618–626 (2012). doi: 10.1093/geronb/gbs067; pmid: 22967933
19. D. H. Sullivan, L. Liu, P. K. Roberson, M. M. Bopp, J. C. Rees, Body weight change and mortality in a cohort of elderly patients recently discharged from the hospital. *J. Am. Geriatr. Soc.* **52**, 1696–1701 (2004). doi: 10.1111/j.1532-5415.2004.52463.x; pmid: 15450047
20. L. Sun, A. A. Sadighi Akha, R. A. Miller, J. M. Harper, Life-span extension in mice by preweaning food restriction and by methionine restriction in middle age. *J. Gerontol. A Biol. Sci. Med. Sci.* **64**, 711–722 (2009). doi: 10.1093/gerona/glp051; pmid: 19414512
21. S. Burgess *et al*., Dissecting causal pathways using Mendelian randomization with summarized genetic data: Application to age at menarche and risk of breast cancer. *Genetics* **207**, 481–487 (2017). doi: 10.1534/genetics.117.300191; pmid: 28835472
22. P. R. Timmers *et al*., Genomics of 1 million parent lifespans implicates novel pathways and common diseases and distinguishes survival chances. *eLife* **8**, e39856 (2019). doi: 10.7554/eLife.39856; pmid: 30642433
23. L. Yengo *et al*., Meta-analysis of genome-wide association studies for height and body mass index in ~700000 individuals of European ancestry. *Hum. Mol. Genet.* **27**, 3641–3649 (2018). doi: 10.1093/hmg/ddy271; pmid: 30124842
24. J. Tyrrell *et al*., Height, body mass index, and socioeconomic status: Mendelian randomisation study in UK Biobank. *BMJ* **352**, i582 (2016). doi: 10.1136/bmj.i582; pmid: 26956984
25. F. W. Albert, L. Kruglyak, The role of regulatory variation in complex traits and disease. *Nat. Rev. Genet.* **16**, 197–212 (2015). doi: 10.1038/nrg3891; pmid: 25707927
26. E. Porcu *et al*., Differentially expressed genes reflect disease-induced rather than disease-causing changes in the transcriptome. *Nat. Commun.* **12**, 5647 (2021). doi: 10.1038/s41467-021-25805-y; pmid: 34561431
27. M. Bou Sleiman *et al*., The gene-regulatory footprint of aging highlights conserved central regulators. *Cell Rep.* **32**, 108203 (2020). doi: 10.1016/j.celrep.2020.108203; pmid: 32997995
28. B. A. Benayoun *et al*., Remodeling of epigenome and transcriptome landscapes with aging in mice reveals widespread induction of inflammatory responses. *Genome Res.* **29**, 697–709 (2019). doi: 10.1101/gr.240093.118; pmid: 30858345
29. A. Tyshkovskiy *et al*., Identification and application of gene expression signatures associated with lifespan extension. *Cell Metab.* **30**, 573–593.e8 (2019). doi: 10.1016/j.cmet.2019.06.018; pmid: 31353263
30. S. T. Gal-Oz *et al*., ImmGen report: Sexual dimorphism in the immune system transcriptome. *Nat. Commun.* **10**, 4295 (2019). doi: 10.1038/s41467-019-12348-6; pmid: 31541153
31. P. Bastard *et al*., Autoantibodies against type I IFNs in patients with life-threatening COVID-19. *Science* **370**, eabd4585 (2020). doi: 10.1126/science.abd4585; pmid: 32972996
32. T. Takahashi *et al*., Sex differences in immune responses that underlie COVID-19 disease outcomes. *Nature* **588**, 315–320 (2020). doi: 10.1038/s41586-020-2700-3; pmid: 32846427
33. J. P. de Magalhães, J. Curado, G. M. Church, Meta-analysis of age-related gene expression profiles identifies common signatures of aging. *Bioinformatics* **25**, 875–881 (2009). doi: 10.1093/bioinformatics/btp073; pmid: 19189975
34. N. Almanzar *et al*., A single-cell transcriptomic atlas characterizes ageing tissues in the mouse. *Nature* **583**, 590–595 (2020). doi: 10.1038/s41586-020-2496-1; pmid: 32669714
35. J. J. Crowley *et al*., Analyses of allele-specific gene expression in highly divergent mouse crosses identifies pervasive allelic imbalance. *Nat. Genet.* **47**, 353–360 (2015). doi: 10.1038/ng.3222; pmid: 25730764
36. S. F. Pinter *et al*., Allelic imbalance is a prevalent and tissue-specific feature of the mouse transcriptome. *Genetics* **200**, 537–549 (2015). doi: 10.1534/genetics.115.176263; pmid: 25858912
37. R. Mott *et al*., The architecture of parent-of-origin effects in mice. *Cell* **156**, 332–342 (2014). doi: 10.1016/j.cell.2013.11.043; pmid: 24439386
38. S. Cleary, C. Seoighe, Perspectives on allele-specific expression. *Annu. Rev. Biomed. Data Sci.* **4**, 101–122 (2021). doi: 10.1146/annurev-biodatasci-021621-122219; pmid: 34465174
39. R. Tacutu *et al*., Human ageing genomic resources: New and updated databases. *Nucleic Acids Res.* **46** (D1), D1083–D1090 (2018). doi: 10.1093/nar/gkx1042; pmid: 29121237
40. A. Battle, C. D. Brown, B. E. Engelhardt, S. B. Montgomery; GTEx Consortium; Laboratory, Data Analysis &Coordinating Center (LDACC)—Analysis Working Group; Statistical Methods groups—Analysis Working Group; Enhancing GTEx (eGTEx) groups; NIH Common Fund; NIH/NCI; NIH/NHGRI; NIH/NIMH; NIH/NIDA; Biospecimen Collection Source Site—NDRI; Biospecimen Collection Source Site—RPCI; Biospecimen Core Resource—VARI; Brain Bank Repository—University of Miami Brain Endowment Bank; Leidos Biomedical—Project Management; ELSI Study; Genome Browser Data Integration &Visualization—EBI; Genome Browser Data Integration &Visualization—UCSC Genomics Institute, University of California Santa Cruz; Lead analysts; Laboratory, Data Analysis &Coordinating Center (LDACC); NIH program management; Biospecimen collection; Pathology; eQTL manuscript working group, Genetic effects on gene expression across human tissues. *Nature* **550**, 204–213 (2017). doi: 10.1038/nature24277; pmid: 29022597
41. E. Porcu *et al*., Mendelian randomization integrating GWAS and eQTL data reveals genetic determinants of complex and clinical traits. *Nat. Commun.* **10**, 3300 (2019). doi: 10.1038/s41467-019-10936-0; pmid: 31341166
42. A. V. Samuelson, C. E. Carr, G. Ruvkun, Gene activities that mediate increased life span of *C. elegans* insulin-like signaling mutants. *Genes Dev.* **21**, 2976–2994 (2007). doi: 10.1101/gad.1588907; pmid: 18006689
43. R. Das *et al*., The homeodomain-interacting protein kinase HPK-1 preserves protein homeostasis and longevity through master regulatory control of the HSF-1 chaperone network and TORC1-restricted autophagy in *Caenorhabditis elegans*. *PLOS Genet.* **13**, e1007038 (2017). doi: 10.1371/journal.pgen.1007038; pmid: 29036198
44. A. J. Dobson *et al*., Longevity is determined by ETS transcription factors in multiple tissues and diverse species. *PLOS Genet.* **15**, e1008212 (2019). doi: 10.1371/journal.pgen.1008212; pmid: 31356597
45. S. P. Curran, G. Ruvkun, Lifespan regulation by evolutionarily conserved genes essential for viability. *PLOS Genet.* **3**, e56 (2007). doi: 10.1371/journal.pgen.0030056; pmid: 17411345
46. C. Y. Ewald, J. N. Landis, J. Porter Abate, C. T. Murphy, T. K. Blackwell, Dauer-independent insulin/IGF-1-signalling implicates collagen remodelling in longevity. *Nature* **519**, 97–101 (2015). doi: 10.1038/nature14021; pmid: 25517099
47. T. Yamagata *et al*., Genome organization of human 48-kDa oligosaccharyltransferase (DDOST). *Genomics* **45**, 535–540 (1997). doi: 10.1006/geno.1997.4966; pmid: 9367678
48. R. D. Semba, E. J. Nicklett, L. Ferrucci, Does accumulation of advanced glycation end products contribute to the aging phenotype? *J. Gerontol. A Biol. Sci. Med. Sci.* **65**, 963–975 (2010). doi: 10.1093/gerona/glq074; pmid: 20478906
49. P. R. H. J. Timmers, J. F. Wilson, P. K. Joshi, J. Deelen, Multivariate genomic scan implicates novel loci and haem metabolism in human ageing. *Nat. Commun.* **11**, 3570 (2020). doi: 10.1038/s41467-020-17312-3; pmid: 32678081
50. L. Mouchiroud *et al*., Pyruvate imbalance mediates metabolic reprogramming and mimics lifespan extension by dietary restriction in *Caenorhabditis elegans*. *Aging Cell* **10**, 39–54 (2011). doi: 10.1111/j.1474-9726.2010.00640.x; pmid: 21040400
51. P. W. Stacpoole, The pyruvate dehydrogenase complex as a therapeutic target for age-related diseases. *Aging Cell* **11**, 371–377 (2012). doi: 10.1111/j.1474-9726.2012.00805.x; pmid: 22321732
52. A. Dillin *et al*., Rates of behavior and aging specified by mitochondrial function during development. *Science* **298**, 2398–2401 (2002). doi: 10.1126/science.1077780; pmid: 12471266
53. R. H. Houtkooper *et al*., Mitonuclear protein imbalance as a conserved longevity mechanism. *Nature* **497**, 451–457 (2013). doi: 10.1038/nature12188; pmid: 23698443
54. T. Lima, T. Y. Li, A. Mottis, J. Auwerx, Pleiotropic effects of mitochondria in aging. *Nat Aging* **2**, 199–213 (2022). doi: 10.1038/s43587-022-00191-2
55. M. A. Aon *et al*., Mitochondrial health is enhanced in rats with higher vs. lower intrinsic exercise capacity and extended lifespan. *NPJ Aging Mech. Dis.* **7**, 1–16 (2021). doi: 10.1038/s41514-020-00054-3; pmid: 33398019
56. P. Hanlon *et al*., Three-locus and four-locus QTL interactions influence mouse insulin-like growth factor-I. *Physiol. Genomics* **26**, 46–54 (2006). doi: 10.1152/physiolgenomics.00247.2005; pmid: 16782841
57. J. M. Harper, S. J. Durkee, R. C. Dysko, S. N. Austad, R. A. Miller, Genetic modulation of hormone levels and life span in hybrids between laboratory and wild-derived mice.

J. Gerontol. A Biol. Sci. Med. Sci. **61**, 1019–1029 (2006). doi: 10.1093/gerona/61.10.1019; pmid: 17077194
58. S. V. Nuzhdin, E. G. Pasyukova, C. L. Dilda, Z.-B. Zeng, T. F. C. Mackay, Sex-specific quantitative trait loci affecting longevity in *Drosophila melanogaster*. *Proc. Natl. Acad. Sci. U.S.A.* **94**, 9734–9739 (1997). doi: 10.1073/pnas.94.18.9734; pmid: 9275193
59. M. Sadagurski, G. Cady, R. A. Miller, Anti-aging drugs reduce hypothalamic inflammation in a sex-specific manner. *Aging Cell* **16**, 652–660 (2017). doi: 10.1111/acel.12590; pmid: 28544365
60. M. Garratt, B. Bower, G. G. Garcia, R. A. Miller, Sex differences in lifespan extension with acarbose and 17-α estradiol: Gonadal hormones underlie male-specific improvements in glucose tolerance and mTORC2 signaling. *Aging Cell* **16**, 1256–1266 (2017). doi: 10.1111/acel.12656; pmid: 28834262
61. R. A. Miller *et al*., Rapamycin-mediated lifespan increase in mice is dose and sex dependent and metabolically distinct from dietary restriction. *Aging Cell* **13**, 468–477 (2014). doi: 10.1111/acel.12194; pmid: 24341993
62. M. Parra-Vargas, M. Ramon-Krauel, C. Lerin, J. C. Jimenez-Chillaron, Size does matter: Litter size strongly determines adult metabolism in rodents. *Cell Metab.* **32**, 334–340 (2020). doi: 10.1016/j.cmet.2020.07.014; pmid: 32814016
63. D. L. Palliyaguru *et al*., Fasting blood glucose as a predictor of mortality: Lost in translation. *Cell Metab.* **33**, 2189–2200.e3 (2021). doi: 10.1016/j.cmet.2021.08.013; pmid: 34508697
64. C. Franceschi, J. Campisi, Chronic inflammation (inflammaging) and its potential contribution to age-associated diseases. *J. Gerontol. A Biol. Sci. Med. Sci.* **69** (Suppl 1), S4–S9 (2014). doi: 10.1093/gerona/glu057; pmid: 24833586
65. J. H. Nadeau, J. Auwerx, The virtuous cycle of human genetics and mouse models in drug discovery. *Nat. Rev. Drug Discov.* **18**, 255–272 (2019). doi: 10.1038/s41573-018-0009-9; pmid: 30679805
66. M. A. Bogue *et al*., Mouse Phenome Database: A data repository and analysis suite for curated primary mouse phenotype data. *Nucleic Acids Res.* **48**, D716–D723 (2020). pmid: 31696236
67. S. Gabriel, L. Ziaugra, D. Tabbaa, SNP genotyping using the Sequenom MassARRAY iPLEX platform. *Curr. Protoc. Hum. Genet.* **60**, 2.12.1–2.12.18 (2009). doi: 10.1002/0471142905.hg0212s60; pmid: 19170031
68. M. Bou Sleiman, Sex- and age-dependent genetics of longevity in a heterogeneous mouse population, Zenodo (2022); https://doi.org/10.5281/zenodo.6625242.

ACKNOWLEDGMENTS

We thank all technical and scientific members of the Interventions Testing Program, who have produced and made the data available. We also thank J.-D. Morel, G. Benegiamo, and L. Goeminne for comments on the manuscript. **Funding:** Ecole Polytechnique Fédérale de Lausanne (J.A.); European Research Council grant ERC-AdG-787702 (J.A.); Swiss National Science Foundation grant 31003A-179435 (J.A.); Swiss National Science Foundation grant 310030-189147 (Z.K.); National Institutes of Health grant AG043930 (R.W., J.A.); National Institutes of Health grant AG022303 (R.M.); National Institutes of Health grant AG022308 (D.H.); National Institutes of Health grant AG022307 (R.S.); Glenn Foundation for Medical Research (R.M.); R.S. is supported by a Senior Research Career Scientist Award from the Department of Veterans Affairs Office of Research and Development. **Author contributions:** Conceptualization: J.A., R.W., R.M. Data curation: S.R., M.B.S. Formal Analysis: M.B.S., M.S., G.V.G.vA. Investigation: M.B.S., A.G., M.S. Methodology: M.B.S., S.R., R.W. Resources: R.M., R.S., J.N., D.H., R.W., J.A. Software: M.B.S. Validation: M.B.S., A.G. Visualization: M.B.S. Web application: M.B.S. Writing – original draft: M.B.S., J.A. Writing – review and editing: M.B.S., J.A., R.W., R.M., Z.K. Funding acquisition: J.A., R.W., R.M., J.N., D.H., R.S. Project administration: R.W., J.A. Supervision: J.A., R.W. **Competing interests:** The authors declare that they have no competing interests. **Data and materials availability:** All data and code are available at Zenodo (*68*). Raw RNA-seq data are available on GEO (GSE194321).

SUPPLEMENTARY MATERIALS

science.org/doi/10.1126/science.abo3191
Materials and Methods
Figs. S1 to S6
Tables S1 and S2
References (*69*–*93*)
Data S1 to S6

View/request a protocol for this paper from *Bio-protocol*.

Submitted 27 January 2022; resubmitted 9 June 2022
Accepted 10 August 2022
10.1126/science.abo3191